A Reduced-order Aggregated Model for Parallel Inverter Systems with Virtual Oscillator Control

M. M. S. Khan, Yashen Lin
National Renewable Energy Laboratory
Golden, Colorado
E-mail: {mohammed.khan,yashen.lin}@nrel.gov

Brian Johnson
Dept. of Electrical Engineering
University of Washington
E-mail: brianbj@uw.edu

Victor Purba, Mohit Sinha, Sairaj Dhople
Dept. of Electrical and Computer Engineering
University of Minnesota
E-mail: {purba002,sinha052,sdhople}@umn.edu

***Abstract*—This paper introduces a reduced-order aggregated model for parallel-connected inverters controlled with virtual oscillator control (VOC). The premise of VOC is to modulate inverter dynamics to emulate those of nonlinear oscillators with the goal of realizing a stable ac microgrid in the absence of communication, synchronous generation, or a stiff grid. To obtain a reduced-order model for a system of parallel-connected inverters with VOC, we first formulate a set of scaling laws that describe how the controller and filter parameters of a given inverter depend on its voltage and power rating. Subsequently, we show that N parallel inverters which adhere to this scaling law can be modeled with the same structure and hence the same computational burden of the model of a single inverter. The proposed aggregate model is experimentally validated on a system of three parallel inverters with heterogeneous power ratings.**

I. Introduction

To facilitate analysis of next-generation systems while taming model complexity, there is a need to obtain reduced-order representations of multi-converter systems that capture their dynamic characteristics with sufficient fidelity. This is true in both grid-connected and islanded (microgrid) systems that may contain large numbers of power electronics interfaces. Towards that end, this paper is focused on the development of a reduced-order aggregated model for collections of parallel connected inverters controlled with a strategy called virtual oscillator control (VOC) [1], [2]. The main idea behind VOC is to modulate inverter dynamics to emulate nonlinear oscillators, which when connected in an electrical network realize a synchronous ac microgrid without external forcing or communication channels. While similar to droop control in application and steady-state performance, VOC is a real-time control strategy, and can be engineered for improved time-domain performance [3], [4].

Since VOC enables decentralized system architectures that are modular and resilient, it is likely to be used in installations that contain large numbers of parallel-connected inverters. Accordingly, systems with VOC are expected to have non-trivial modeling complexity associated with them and it is necessary to develop modeling approaches that facilitate their analysis. We formulate a reduced-order aggregated model for N parallel-connected VOC inverters with heterogeneous power ratings. In particular, we show that if the control and physical parameters of each inverter adhere to a set of scaling laws (see Fig. 1a), then the dynamics of a multi-inverter system can be modeled exactly as one aggregated equivalent inverter model (see Fig. 1b). Hence, the proposed modeling approach reduces modeling complexity by a factor of $1/N$ while preserving the dynamic response at the system output terminals.

Traditionally, the majority of work on aggregate models has been focused on bulk systems where machine dynamics are of particular interest [5]–[8]. Literature pertinent in theme and application to the present work relates to reduced-order models for collections of droop-controlled inverters [9]–[11] and machines [12]–[14]. An impedance-based analysis was applied in [15] to obtain an aggregate model for collections of identical grid-connected inverters with current control. Along similar lines, a lumped-parameter and time-domain reduced-order model was recently proposed [16], [17] for systems of grid-following inverters (i.e., inverters controlled with a phase-locked loop and current control). There are also reduced-order models of droop-controlled inverters in islanded settings [18]–[20].

Although the formulation in [16] is inspirational since we leverage a similar set of scaling laws, our contribution here is distinct since we analyze a fundamentally different controller, namely VOC, for microgrid applications. This paper offers the following unique contributions in comparison to existing literature: i) we formulate a set of scaling laws that are applicable individual to inverters with VOC, ii) we prove that N heterogeneous inverters that adhere to the proposed scaling laws can be modeled as a single aggregated equivalent inverter whose physical and control structure mirrors that of an individual inverter (albeit with some parametric scalings), iii) the analytical model is simulated and compared to measurements from a multi-inverter hardware setup, and iv) a sensitivity study shows our aggregated model is robust to parameter mismatch. Taken together with prior reduced-order modeling methods for droop-controlled inverters, and grid-following inverters, this paper adds to the literature on modeling of complex power-electronics systems.

The remainder of this paper is structured as follows: The

978-1-5386-5541-2/18/$31.00

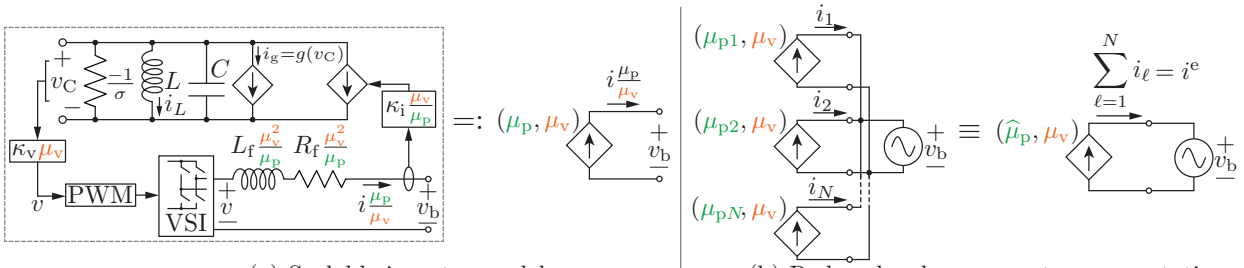

(a) Scalable inverter model (b) Reduced order aggregate representation

Fig. 1: (a) Diagram of scalable model for a single inverter with VOC, where μ_p and μ_v are the power and voltage scaling factors, respectively. (b) A system of N parallel VO-controlled inverters with heterogeneous power ratings can be modeled equivalently as an aggregated inverter with the same model structure as any individual inverter.

VOC control strategy and inverter model are introduced in Section II. In Section III, we define the proposed scaling laws and show that N parallel inverters with VOC can be modeled as an aggregated equivalent. Experimental results are given in Section IV and concluding remarks are in Section V.

II. Unscaled VOC Inverter Model

In this section, we describe the unscaled VOC inverter model. This will be subsequently leveraged to derive the scaled model and the aggregation result.

A. Description of Inverter Model and Controller

In order to scale the VOC inverter to the required power and voltage ratings, we begin by introducing power- and voltage-scaling factors, μ_p, and μ_v, respectively that will be applied in scaling different controller gains and parameters in the inverters (formally introduced in the next section). First, consider the *unscaled* model of an inverter controlled with VOC. This system is illustrated in Fig. 1a for the case where the power and voltage scaling factors are set to unity (i.e., $\mu_p = \mu_v = 1$). The inverter model includes a single-phase power stage with an RL filter (L_f, and R_f) and a closed-loop controller that realizes a discretized version of the nonlinear oscillator dynamics for control. The oscillator-based controller contains: i) a harmonic LC oscillator with resonant frequency $\omega^* = 1/\sqrt{LC}$, ii) a nonlinear voltage-dependent current source, $g(v_C)$, where v_C is the voltage across the capacitor, and iii) a negative conductance element, $-\sigma$. The virtual oscillator is coupled to the power stage through the voltage and current gains, κ_v, and κ_i, respectively. In particular, the inverter output current, i, is multiplied by κ_i and this is then extracted from the virtual oscillator circuit, i.e, the signal, $\kappa_i i$ is passed to the virtual oscillator circuit as the input. The output voltage of the virtual capacitor, v_C is scaled by κ_v to obtain the voltage command v. We assume that the commanded voltage, v, appears at the H-bridge terminals via pulse width modulation (PWM).

B. Dynamics of Inverter Model

The dynamics of the virtual inductor current, i_L, and capacitor voltage, v_C, are

$$\begin{aligned} \dot{i}_L &= \frac{1}{L} v_C, \\ \dot{v}_C &= \frac{1}{C}\left(-g(v_C) + \sigma v_C - i_L - \kappa_i i\right), \end{aligned} \tag{1}$$

where $g : \mathbb{R} \to \mathbb{R}$ is constructed to satisfy the following conditions in Liénard's theorem for existence of a unique, stable limit cycle [21]:

1) $g(v_C)$ is continuously differentiable $\forall v_C$,
2) $g(v_C)$ is an odd function (i.e. $g(-v_C) = -g(v_C), \forall v_C$),
3) $g(v_C) > 0$ for $v_C > 0$.

In addition to this, we assume that

$$g(x) - g(y) = (x - y)\, f(x, y), \ \forall x, y,$$

for some real-valued function $f(x, y)$. Lastly, the dynamics of the output filter are described by

$$\dot{i} = \frac{1}{L_f}\left(-R_f i + \kappa_v v_C - v_b\right), \tag{2}$$

where v_b is the AC bus voltage. Equations (1) and (2) consist the dynamics of the unscaled VOC inverter.

III. Inverter Scaling and Aggregate Model for Multi-Inverter System

In this section, we begin by formally defining the power- and voltage-scaling factors of the VOC inverter model, and establishing the relationship between the states in the scaled and unscaled models. After specifying the proposed scaling law, we present the main result on inverter aggregation for parallel-connected inverters as illustrated in Fig. 1b.

A. Scaling of inverter

The *power scaling* factor μ_p, and the *voltage-scaling* factor μ_v, are defined as

$$\mu_p := \frac{p_{\text{rated}}}{p_{\text{base}}}, \quad \mu_v := \frac{v_{\text{rated}}}{v_{\text{base}}}, \tag{3}$$

where p_{rated} and v_{rated} are the rated power and voltage, respectively, of a given inverter, and p_{base} and v_{base} are system-wide base values (they may be assumed to be the ratings of a

nominal unscaled inverter). As shown in Fig. 1a, we obtain the scaled inverter model by modifying the following parameters:

$$(\kappa_{\rm v}, \kappa_{\rm i}, R_{\rm f}, L_{\rm f}) \to \left(\kappa_{\rm v}\mu_{\rm v}, \kappa_{\rm i}\frac{\mu_{\rm v}}{\mu_{\rm p}}, R_{\rm f}\frac{\mu_{\rm v}^2}{\mu_{\rm p}}, L_{\rm f}\frac{\mu_{\rm v}^2}{\mu_{\rm p}}\right). \quad (4)$$

Let $i_{\rm L}^{\rm s}, v_{\rm C}^{\rm s}, i^{\rm s}$ be the virtual-oscillator inductor current, virtual-oscillator capacitor voltage, and output current of the scaled inverter, respectively. The dynamics for the scaled inverter are given by:

$$\dot{i}_{\rm L}^{\rm s} = \frac{1}{L}v_{\rm C}^{\rm s}, \quad (5)$$

$$\dot{v}_{\rm C}^{\rm s} = \frac{1}{C}\left(-g(v_{\rm C}^{\rm s}) + \sigma v_{\rm C}^{\rm s} - i_{\rm L}^{\rm s} - \frac{\mu_{\rm v}}{\mu_{\rm p}}\kappa_i i^{\rm s}\right), \quad (6)$$

$$\dot{i}^{\rm s} = \frac{\mu_{\rm p}}{\mu_{\rm v}^2 L_{\rm f}}\left(-\frac{\mu_{\rm v}^2}{\mu_{\rm p}}R_{\rm f} i^{\rm s} + \mu_{\rm v}\kappa_{\rm v} v_{\rm C}^{\rm s} - \mu_{\rm v} v_{\rm b}\right). \quad (7)$$

The relationship between the states in the scaled and unscaled inverter models is established below.

Proposition 1 (*Scaled Inverter Model*). Consider the dynamical model for the unscaled VOC inverter in (1)–(2), and for the scaled VOC inverter in (5)–(7). Suppose the initial conditions at $t_0 \geq 0$ are such that $i_{\rm L}^{\rm s}(t_0) = i_{\rm L}(t_0)$, $v_{\rm C}^{\rm s}(t_0) = v_{\rm C}(t_0)$, and $i^{\rm s}(t_0) = \frac{\mu_{\rm p}}{\mu_{\rm v}} i(t_0)$. Then, we have $\forall t \geq t_0$

$$i_{\rm L}^{\rm s}(t) = i_{\rm L}(t), \quad v_{\rm C}^{\rm s}(t) = v_{\rm C}(t), \quad i^{\rm s}(t) = \frac{\mu_{\rm p}}{\mu_{\rm v}} i(t). \quad (8)$$

Proof. Define $x := [i_{\rm L}, v_{\rm C}, i]^{\rm T}$, $x^{\rm s} := [i_{\rm L}^{\rm s}, v_{\rm C}^{\rm s}, i^{\rm s}]^{\rm T}$, and *scaling vector* $\eta := [1, 1, \frac{\mu_{\rm p}}{\mu_{\rm v}}]^{\rm T}$. We also define $z := x^{\rm s} - {\rm diag}(\eta)x$, with z_ℓ denoting the ℓ-th entry of z. The dynamics of z are given by

$$\dot{z}_1 = \dot{i}_{\rm L}^{\rm s} - \dot{i}_{\rm L} = \frac{1}{L}v_{\rm C}^{\rm s} - \frac{1}{L}v_{\rm C} = \frac{1}{L}z_1, \quad (9)$$

$$\begin{aligned}\dot{z}_2 = \dot{v}_{\rm C}^{\rm s} - \dot{v}_{\rm C} &= \frac{1}{C}\left(-g(v_{\rm C}^{\rm s}) + \sigma v_{\rm C}^{\rm s} - i_{\rm L}^{\rm s} - \frac{\mu_{\rm v}}{\mu_{\rm p}}\kappa_i i^{\rm s}\right) \\ &\quad - \frac{1}{C}\left(-g(v_{\rm C}) + \sigma v_{\rm C} - i_{\rm L} - \kappa_i i\right) \\ &= -\frac{1}{C}\underbrace{\left(g(v_{\rm C}^{\rm s}) - g(v_{\rm C})\right)}_{=:h(z_2)} + \frac{\sigma}{C}z_2 - \frac{1}{C}z_1 - \frac{\mu_{\rm v}}{\mu_{\rm p}C}\kappa_i z_3, \quad (10)\end{aligned}$$

$$\begin{aligned}\dot{z}_3 = \dot{i}^{\rm s} - \frac{\mu_{\rm p}}{\mu_{\rm v}}\dot{i} &= \frac{\mu_{\rm p}}{\mu_{\rm v}^2 L_{\rm f}}\left(-\frac{\mu_{\rm v}^2}{\mu_{\rm p}}R_{\rm f} i^{\rm s} + \mu_{\rm v}\kappa_{\rm v} v_{\rm C}^{\rm s} - \mu_{\rm v} v_{\rm b}\right) \\ &\quad - \frac{\mu_{\rm p}}{\mu_{\rm v} L_{\rm f}}\left(-R_{\rm f} i + \kappa_{\rm v} v_{\rm C} - v_{\rm b}\right) \\ &= -\frac{R_{\rm f}}{L_{\rm f}}z_3 + \frac{\mu_{\rm p}\kappa_v}{\mu_{\rm v} L_{\rm f}}z_2, \quad (11)\end{aligned}$$

where $h(z_2) = 0$ when $z_2 = 0$. If we initialize $z(t_0) = x^{\rm s}(t_0) - {\rm diag}(\eta)x(t_0) = 0_3$, we have $z(t) = 0_3, \forall t \geq t_0$. By the definition of z, we have $i_{\rm L}^{\rm s}(t) = i_{\rm L}(t)$, $v_{\rm C}^{\rm s}(t) = v_{\rm C}(t)$, $i^{\rm s}(t) = \frac{\mu_{\rm p}}{\mu_{\rm v}} i(t)$, $\forall t \geq t_0$. □

This result implies that the scalings do not affect the inherent dynamical behavior of the virtual-oscillator states, while the current of the output filter is exactly scaled by the ratio of the inverter rated current and the system-wide base value for the current (see the definition of $\mu_{\rm p}$ and $\mu_{\rm v}$ in (3)).

B. Aggregation of Parallel-connected Inverters

Now, consider a collection of parallel inverters with heterogeneous power ratings. This is mathematically captured by ascribing the (different) power-scaling factors $\mu_{\rm p1}, \ldots, \mu_{{\rm p}N}$ to inverters in the multi-inverter system as illustrated in Fig. 1b. Since all inverters are parallel connected, we assume they have the same voltage rating, i.e. $\mu_{\rm v1} = \ldots = \mu_{{\rm v}N} =: \mu_{\rm v}$. Define the equivalent power-scaling factor as $\widehat{\mu}_{\rm p} := \sum_{\ell=1}^{N}\mu_{{\rm p}\ell}$. The relationship between the aggregated output current, denoted as $i^{\rm e}$, and the net current produced by the multi-inverter system is specified below.

Proposition 2 (*Reduced-order Aggregate Model*). Let i_ℓ denote the output current of the ℓ-th inverter. The equivalent output current of the reduced order aggregated inverter model, $i^{\rm e}$ is given by

$$i^{\rm e}(t) = \sum_{\ell=1}^{N} i_\ell(t), \quad \forall t \geq t_0. \quad (12)$$

Proof. Recall i is the current of the unscaled model. Using the definition of $\widehat{\mu}_{\rm p}$ and the scaling of output currents in Proposition 1, it follows $\forall t \geq t_0$ that:

$$i^{\rm e}(t) = \frac{\widehat{\mu}_{\rm p}}{\mu_{\rm v}} i(t) = \sum_{\ell=1}^{N}\frac{\mu_{{\rm p}\ell}}{\mu_{\rm v}} i(t) = \sum_{\ell=1}^{N} i_\ell(t).$$

The above equation establishes the reduced-order aggregated model for the parallel connected VOC inverters, and it is illustrated in Fig. 1b. □

IV. Experimental Validation

To validate the proposed modeling framework, we will compare waveforms obtained from the simulated reduced-order inverter model to measurements obtained from a multi-inverter hardware setup. We present two sets of experiments in this section. In the first set, which we will call the nominal case, all the parameters of the individual inverters follow the scaling law. In the second set, we study the robustness of our model to parameter mismatch by varying the filter parameters of one inverter so that it does not follow the scaling law.

A. Experimental setup

The experimental system consists of three inverters ($N = 3$) where each converter has a F28335 DSP controller and a switching frequency of 25 kHz with unipolar PWM. Inverters 1, 2, and 3 have power ratings of approximately 50 W, 50 W, and 25 W, respectively, and we arbitrarily pick the power base value as $p_{\rm base} = 50$ W. As specified above, this implies power scaling factors of $\mu_{\rm p1} = 1$, $\mu_{\rm p2} = 1$, and $\mu_{\rm p3} = 0.5$ for the multi-inverter system (it is worth noting that this natively ensures proportional power sharing [1]), and $\widehat{\mu}_{\rm p} = 2.5$ for the aggregated equivalent inverter. In order to maintain identical voltages at the load side, the voltage-scaling parameters are kept the same for all inverters such that: $\mu_{\rm v} = 1$. The base parameters utilized in the hardware are given in Table I. The voltage-dependent current source, $g(v_{\rm C})$ is chosen as a

deadzone nonlinearity which is parameterized by $\alpha, \varphi \in \mathbb{R}^+$, and defined as [1]:

$$g(v_{\mathrm{C}}) = f(v_{\mathrm{C}}) - \alpha v_{\mathrm{C}}, \tag{13}$$

where $f(v_{\mathrm{C}})$ is a dead-zone function with slope 2α :

$$f(v_{\mathrm{C}}) = \begin{cases} 2\alpha(v_{\mathrm{C}} - \varphi), & v_{\mathrm{C}} > \varphi \\ 0, & |v_{\mathrm{C}}| \leq \varphi \\ 2\alpha(v_{\mathrm{C}} + \varphi), & v_{\mathrm{C}} < -\varphi. \end{cases} \tag{14}$$

TABLE I: Virtual-oscillator control parameters.

Symbol	Value	Units
ω_{nom}	$2\pi 60$	rad/s
κ_{v}	63	V/V
κ_{i}	1.1875	A/A
σ	0.9	S
α	1	$\mathrm{A/V^3}$
φ	0.4695	V
C	0.1759	F
L	39.9	μH
L_f	6	mH
R_f	1	Ω

The aggregated model simulation is developed according to the two propositions described in Section III. The dynamics of the model are given by (5)–(7) with the scaling factor $\mu_{\mathrm{p}} = \widehat{\mu}_{\mathrm{p}} = 2.5$ and $\mu_{\mathrm{v}} = 1$. The corresponding equivalent current is given by:

$$i^{\mathrm{e}}(t) = \frac{\widehat{\mu}_{\mathrm{p}}}{\mu_{\mathrm{v}}} i(t) = 2.5 i_1(t), \tag{15}$$

where $i_1(t)$ is the output current of inverter 1.

B. Nominal Case

In Fig. 2 we provide the measured waveforms alongside the simulated waveforms of the aggregate inverter model during load step changes. Fig. 2a shows a load step up event and Fig. 2b shows a load step down event. The top plots show the measured currents from each individual inverter. The middle plots show the total measured current output from the experiment and the equivalent inverter current from the aggregated model simulation. The bottom plots show the voltage of the experimental and aggregated model simulation. From the plots, we observe that, both before and after the load step change, the equivalent current from our model is consistent with the total measured current output of the three inverters, validating the propositions. The results in Fig. 2a and 2b also show that our model performs well in both the step-up and step-down events.

C. Impact of Filter Parameters

The aggregated model is developed based on the assumption that each individual inverter has filter and control parameters that follow the scaling law of Proposition 1. In practice, this assumption may not hold. (Indeed, although the control parameters can be programed to follow the scaling law, the filter parameters of different inverter may not exactly follow

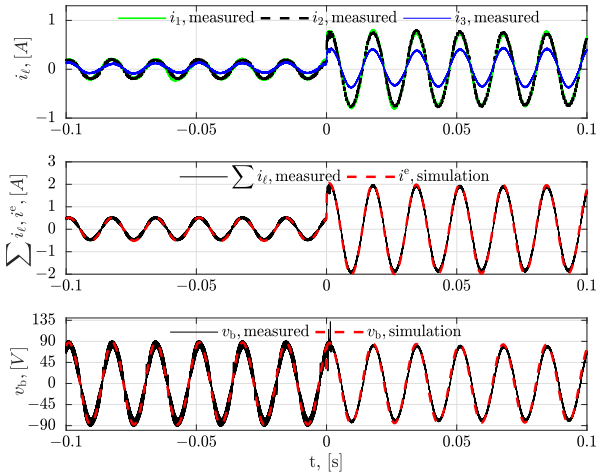

(a) Load step up at $t = 0$.

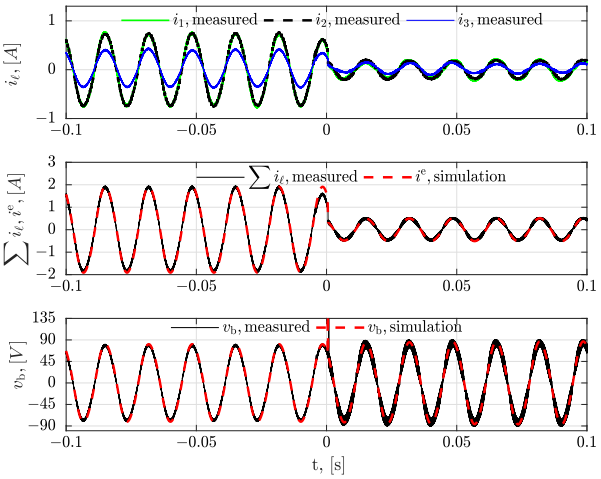

(b) Load step down at $t = 0$.

Fig. 2: Comparison of measurements obtained for a multi-inverter hardware system and simulated waveforms from the reduced-order aggregated inverter model. Waveforms during a load step-up and step-down are shown in (a) and (b), respectively. Top plots shows the measured currents from each individual inverters; the middle plots show the measured total current and the aggregated equivalent current; the bottom plots show the bus voltages for the experimental and simulated systems.

the scaling the law.) In order to show the impact of filter-parameter mismatch on the performance of our aggregated model, we run another set of experiments, where we changed the filter parameters of the third inverter (rated at 25 W). Instead of using the nominal filter parameters ($L_f = 12\,\mathrm{mH}$, and $R_f = 2\,\Omega$) according to the scaling the law as stated in (4), the filter parameters are reduced by half ($L_f = 6\,\mathrm{mH}$, and $R_f = 1\,\Omega$).

We ran the same load step-change experiments as the base case with the modified filter parameters. The results are shown in Fig. 3. We observed that the equivalent current from our

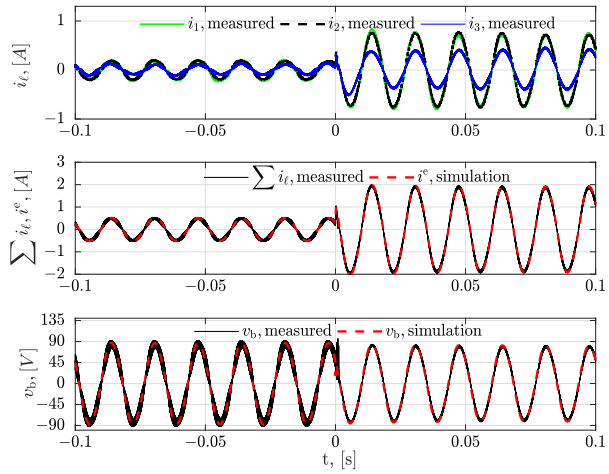

(a) Load step up at $t = 0$.

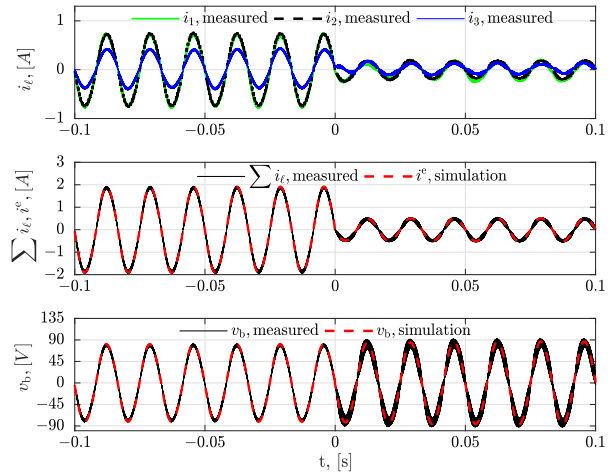

(b) Load step down at $t = 0$.

Fig. 3: Comparison of waveforms of the multi-inverter system and reduced-order inverter model with the filter parameters of inverter 3 reduced in half. Waveforms during a load step-up and step-down are shown in (a) and (b), respectively.

aggregated model is still consistent with the total current from experiment measurements, even with the filter parameters being changed significantly. The model yields accurate results both before and after the step changes, as well as both load step-up and step-down events. This indicates that the proposed model is robust to parameter mismatch.

To quantify the impact of filter-parameter mismatch on the aggregated model, we calculated the root mean square error (RMSE) of the total measured current between the nominal case and the case with reduced filter parameters. The measurements are passed through a low pass filter with a cutoff frequency of 600Hz to get rid of the switching ripple. The filtered total currents are used to calculate the RMSE for both cases; shown in Table II. The results show that the RMSE are very small which indicates that the aggregated model is robust to parameter mismatch.

TABLE II: RMSE of the total measured currents between the nominal case and and the case with reduced filter parameters.

Cases	Changes	RMSE
step up	before step change	0.0341
	after step change	0.0357
step down	before step change	0.0306
	after step change	0.0364

V. Conclusions

Power electronics that work in low inertia power systems are becoming increasingly important. In this paper, we developed a reduced-order model to capture the dynamics of an aggregation of heterogeneous parallel-connected inverters controlled with virtual oscillator control (VOC). The proposed model significantly reduces the model complexity of multi-inverter systems while maintaining reasonable fidelity. The model provides a building block for analyzing complex systems composed of many VOC inverters. In future studies, we also aim to extend the model for the system of inverters with arbitrary electrical networks.

Acknowledgments

This work was supported in part by the: i) Alliance for Sustainable Energy, LLC, the Manager and Operator of the National Renewable Energy Laboratory for the U.S. Department of Energy (DOE) under Contract No. DE-AC36-08GO28308. Funding provided by U.S. Department of Energy Office of Energy Efficiency and Renewable Energy Solar Energy Technologies Office; and ii) National Science Foundation through grants 1453921 and 1509277. The views expressed in the article do not necessarily represent the views of the DOE or the U.S. Government. The U.S. Government retains and the publisher, by accepting the article for publication, acknowledges that the U.S. Government retains a nonexclusive, paidup, irrevocable, worldwide license to publish or reproduce the published form of this work, or allow others to do so, for U.S. Government purposes.

References

[1] B. Johnson, S. Dhople, A. Hamadeh, and P. Krein, "Synchronization of parallel single-phase inverters with virtual oscillator control," *IEEE Trans. Power Electron.*, vol. 29, pp. 6124–6138, Nov. 2014.

[2] L. A. B. Tôrres, J. P. Hespanha, and J. Moehlis, "Power supplies dynamical synchronization without communication," in *Proc. of the Power & Energy Society 2012 General Meeting*, July 2012.

[3] B. Johnson, M. Rodriguez, M. Sinha, and S. Dhople, "Comparison of virtual oscillator and droop control," in *2017 IEEE 18th Workshop on Control and Modeling for Power Electronics (COMPEL)*, pp. 1–6, July 2017.

[4] M. Sinha, F. Dörfler, B. B. Johnson, and S. V. Dhople, "Uncovering droop control laws embedded within the nonlinear dynamics of van der pol oscillators," *IEEE Transactions on Control of Network Systems*, vol. 4, pp. 347–358, June 2017.

[5] A. J. Germond and R. Podmore, "Dynamic aggregation of generating unit models," *IEEE Transactions on Power Apparatus and Systems*, vol. PAS-97, pp. 1060–1069, July 1978.

[6] J. H. Chow, *Power System Coherency and Model Reduction*. Springer, 2013.

[7] S. D. Pekarek, M. T. Lemanski, and E. A. Walters, "On the use of singular perturbations to neglect the dynamic saliency of synchronous machines," *IEEE Transactions on Energy Conversion*, vol. 17, pp. 385–391, September 2002.

[8] H. You, V. Vittal, and X. Wang, "Slow coherency-based islanding," *IEEE Transactions on Power Systems*, vol. 19, pp. 483–491, February 2004.

[9] P. J. Hart, R. H. Lasseter, and T. M. Jahns, "Reduced-order harmonic modeling and analysis of droop-controlled distributed generation networks," in *IEEE 7th International Symposium on Power Electronics for Distributed Generation Systems (PEDG)*, pp. 1–9, June 2016.

[10] K. Kodra, N. Zhong, and Z. Gajić, "Model order reduction of an islanded microgrid using singular perturbations," in *American Control Conference (ACC)*, pp. 3650–3655, July 2016.

[11] P. J. Hart, R. H. Lasseter, and T. M. Jahns, "Enforcing coherency in droop-controlled inverter networks through use of advanced voltage regulation and virtual impedance," in *2017 IEEE Energy Conversion Congress and Exposition (ECCE)*, pp. 3367–3374, October 2017.

[12] J. H. Chow, R. Galarza, P. Accari, and W. W. Price, "Inertial and slow coherency aggregation algorithms for power system dynamic model reduction," *IEEE Transactions on Power Systems*, vol. 10, pp. 680–685, May 1995.

[13] M. L. Ourari, L. A. Dessaint, and V.-Q. Do, "Dynamic equivalent modeling of large power systems using structure preservation technique," *IEEE Transactions on Power Systems*, vol. 21, pp. 1284–1295, August 2006.

[14] A. M. Miah, "Study of a coherency-based simple dynamic equivalent for transient stability assessment," *IET Generation, Transmission Distribution*, vol. 5, pp. 405–416, April 2011.

[15] M. Lu, X. Wang, P. C. Loh, and F. Blaabjerg, "Interaction and aggregated modeling of multiple paralleled inverters with lcl filter," in *2015 IEEE Energy Conversion Congress and Exposition (ECCE)*, pp. 1954–1959, Sept 2015.

[16] V. Purba, S. V. Dhople, S. Jafarpour, F. Bullo, and B. B. Johnson, "Reduced-order structure-preserving model for parallel-connected three-phase grid-tied inverters," in *Workshop on Control and Modeling for Power Electronics*, pp. 1–7, July 2017.

[17] V. Purba, S. V. Dhople, S. Jafarpour, F. Bullo, and B. B. Johnson, "Network-cognizant model reduction of grid-tied three-phase inverters," in *Allerton Conference on Communication, Control, and Computing*, pp. 157–164, Oct. 2017.

[18] L. Luo and S. V. Dhople, "Spatiotemporal model reduction of inverter-based islanded microgrids," *IEEE Transactions on Energy Conversion*, vol. 29, pp. 823–832, December 2014.

[19] M. Rasheduzzaman, J. A. Mueller, and J. W. Kimball, "Reduced-order small-signal model of microgrid systems," *IEEE Transactions on Sustainable Energy*, vol. 6, pp. 1292–1305, October 2015.

[20] O. O. Ajala, A. D. Domínguez-García, and P. W. Sauer, "A hierarchy of models for inverter-based microgrids," in *Energy Markets and Responsive Grids: Modeling, Control and Optimization* (S. Meyn, T. Samad, S. Glavaski, I. Hiskens, and J. Stoustrup, eds.), Berlin: Springer-Verlag, 2017.

[21] S. H. Strogatz, *Nonlinear Dynamics and Chaos: With Applications to Physics, Biology, Chemistry, and Engineering*. Studies in nonlinearity, Westview Press, 1 ed., Jan. 2001.